Dioxygen Replacement Reaction in Myoglobin†

D. Beece, L. Eisenstein, H. Frauenfelder,* D. Good, M. C. Marden, L. Reinisch, A. H. Reynolds, L. B. Sorensen, and K. T. Yue

ABSTRACT: The replacement reaction of myoglobin (Mb), $MbCO + O_2 \rightarrow MbO_2 + CO \rightarrow MbCO + O_2$, has been studied with flash photolysis in the temperature range from 140 to 320 K and the time range from 2 μs to 200 s. In a fraction of the Mb, the photodissociated CO remains within the protein; rebinding is not affected by the presence of O_2 and occurs with rates that are identical with the ones observed earlier in solvents containing only CO. In the remaining fraction CO migrates into the solvent and Mb combines preferentially with oxygen. The rate of the subsequent replacement of O_2 by CO permits calculation of the oxygen dissociation rate k_{O_2}; k_{O_2} has been determined from 260 to 320 K. The measurements support a multibarrier model.

Flash Photolysis Replacement Reactions

The binding of CO and O_2 to myoglobin is one of the simplest biological processes. In previous papers (Austin et al., 1975; Alberding et al., 1978) we investigated ligand binding from 10 to 320 K and introduced a multibarrier model that explains all observed phenomena. The model implies that access of a small ligand to the binding site at the heme iron is not via a random path through a statistical molecular sieve but proceeds along one or a few well-defined pathways. The model is consistent with trajectory calculations (Case & Karplus, 1979). In the present paper we present experiments on replacement reactions after flash photolysis that also support a multibarrier model.

In a typical replacement experiment (Antonini & Brunori, 1971) two solutions, one containing MbO_2 and the other containing known concentrations of O_2 and CO, are mixed in a stopped-flow system. Since CO is much more tightly bound than O_2, the overall reactions shown in eq 1 take place.

$$MbO_2 + CO \rightarrow Mb + O_2 + CO \rightarrow MbCO + O_2 \quad (1)$$

Stopped-flow is not the only technique that permits initiation of a replacement reaction; as early as 1959, Gibson used a photoflash (Gibson, 1959). Such an approach offers many advantages. Mixing techniques are limited to reaction times that are longer than about 1 ms and are difficult or impossible to use with high viscosity solvents or at low temperatures. Flash photolysis also has the advantage that measurements can be repeated with the same sample. Despite these advantages, most experiments have been performed by using stopped-flow. In the present paper, we demonstrate that flash photolysis replacement reactions permit studies over an extended temperature range and provide information on the competition between CO and O_2 for binding sites at temperatures where multiple processes are observed.

Model and Predictions

Some of the essential features of our model (Austin et al., 1975) are shown in Figure 1. Access of CO to the binding site A at the heme iron in Mb is governed by four barriers between A and the solvent S. The Gibbs energy profiles at three temperatures, 50, 215, and 310 K, are given in Figure 1a. For O_2, three barriers separate the binding site A and the solvent S as shown in Figure 1b. Consider Mb in a solvent with, say, equal concentrations of O_2 and CO and with $[Mb] \ll [O_2] = [CO]$. Since CO is more tightly bound than O_2, in equilibrium essentially all binding sites A will be occupied with CO. After a light pulse breaks the bond between Fe and CO, the ligand moves from well A to B in Figure 1a. Rebinding is now determined by the various barriers. The rate coefficient k_{BA} for the transition from B to A, for instance, is given by the Gibbs activation energy $G^{\ddagger}_{BA}$ (the Gibbs energy difference between the bottom of well B and the top of the barrier between B and A) as $k_{BA} = \nu \exp(-G^{\ddagger}_{BA}/RT)$, where $\nu = 10^{13}$ s^{-1} and $R = 8.31$ J K^{-1} mol^{-1} is the gas constant. Rebinding B → A and transitions from B toward the solvent S compete. A fraction N^{out} of all CO molecules moves into the solvent and $1 - N^{out}$ rebinds without ever leaving the protein. [Details are described by Austin et al. (1975).] All CO and O_2 molecules in the solvent will compete for the fraction N^{out} of free binding sites. Since O_2 reaches the binding site much faster than CO, nearly all of the free Mb will initially bind O_2. The bound O_2 will thermally dissociate with a rate coefficient k_{O_2}, and O_2 and CO again compete for the vacant site. In each try, O_2 is favored, but once CO reaches a free binding site it will remain there since $k_{CO} \ll k_{O_2}$. (At 293 K, $k_{CO} \simeq 0.02$ s^{-1} and $k_{O_2} \simeq 10$ s^{-1}.) The main branches of the overall processes thus can be described as shown in eq 2. We

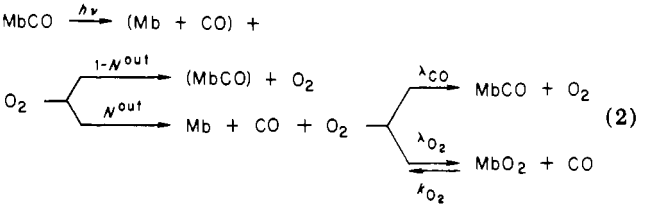

(2)

denote with λ_{CO} the pseudo-first-order rate coefficient for binding of CO to Mb from a solvent in which there is no competing O_2 present; λ_{O_2} has the corresponding meaning for a CO-free solvent. With Figure 1, the features expected at various temperatures can now be predicted. Below about 180 K, the CO in well B after the photodissociation encounters large Gibbs energy barriers toward the solvent and will always rebind. N^{out} is zero and no replacement takes place. At 215 K, the barriers still favor rebinding from the inside of the protein. N^{out} thus is small, and only a small fraction of Mb molecules participates in the replacement reaction. At 310 K, N^{out} is essentially equal to one; only a small fraction of CO rebinds directly, and nearly all Mb participates in the re-

† From the Department of Physics, University of Illinois at Urbana–Champaign, Urbana, Illinois 61801. *Received April 10, 1979.* This work was supported in part by the U.S. Department of Health, Education and Welfare under Grant GM 18051 and the National Science Foundation under Grant PCM 76-81025.

0006-2960/79/0418-3421$01.00/0

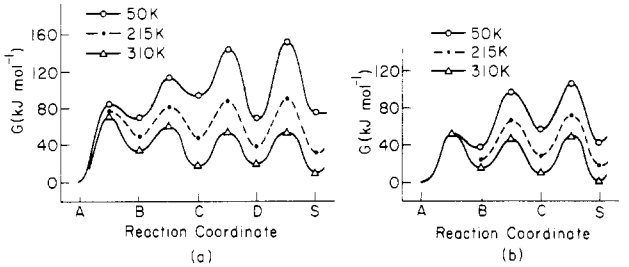

FIGURE 1: Gibbs energy at T = 50, 215, and 310 K as a function of reaction coordinate for (a) MbCO, [CO] = 150 μM, and (b) MbO_2, [O_2] = 200 μM, in glycerol–water (Austin et al. 1975).

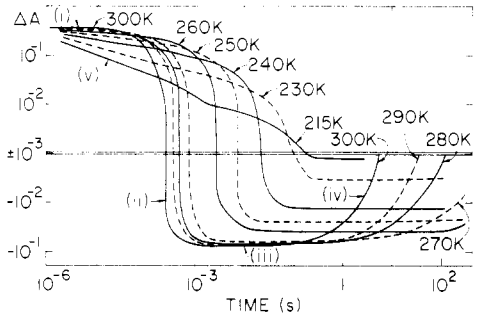

FIGURE 2: Recombination kinetics of a 40 μM Mb sample equilibrated with 0.5 bar of CO and 0.5 bar of O_2. Solvent was glycerol–water (3:1, v/v) with 50 mM phosphate buffer, pH 7. With respect to the MbCO center line, ΔA is positive for deoxy Mb and negative for MbO_2. The main features labeled are (i) deoxy Mb, (ii) binding of O_2, (iii) MbO_2, (iv) replacement of O_2 by CO, and (v) direct rebinding of CO via intramolecular processes.

placement reaction. We will show in the following that these predictions are verified by the experiment.

Experimental Approach and Results

The flash photolysis experiments were performed with the apparatus described earlier (Austin et al., 1975, 1976), consisting of a 1-μs dye laser, a logarithmic transient recorder, and a cryostat.

Samples of sperm whale Mb in glycerol–water (3:1, v/v) and 50 mM phosphate buffer at pH 7 were equilibrated with 1 bar of CO. After reduction by a 2:1 excess of dithionite, the sample was equilibrated with 1 bar of a CO–O_2 mixture for at least 3 h. A sample cell of 1-cm optical path length was used to keep the Mb concentration (10 μM) much less than that of CO or O_2. A 2-mm cell with 40 μM Mb provided better light transmission at low temperatures. The reactions were monitored at 436 nm, where the extinction coefficients are 1.2×10^5 M^{-1} cm^{-1} for Mb, 5×10^4 M^{-1} cm^{-1} for MbCO, and 4×10^4 M^{-1} cm^{-1} for MbO_2. The absorbance after photodissociation was measured from 2 μs to 200 s over the temperature range from 140 to 320 K. At temperatures where the replacement reaction time exceeds 10 s, the sample was warmed between measurements to insure an initial state of MbCO.

The results shown in Figure 2 are for a 40 μM Mb sample equilibrated with 0.5 bar of CO and 0.5 bar of O_2. The plot represents the log of the absorbance change vs. the log of the time after photodissociation. The zero of the absorbance refers to MbCO. The absorbance change is positive for Mb and negative for MbO_2. To accommodate both positive and negative values of ΔA on the log scale, we cut the scale and omitted the (infinite) part between $+10^{-3}$ and -10^{-3}. (The easiest way to produce the proper graph paper is to start with two pages of log–log paper, turn the second by 90°, and paste them together.) For the following discussion, we have labeled

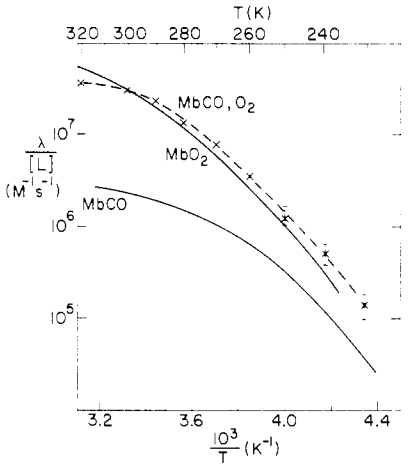

FIGURE 3: Second-order rate coefficient $\lambda'/[O_2]$ for the process labeled ii in Figure 2, [O_2] = 200 μM. Also shown as solid lines are the rate coefficients $\lambda_{CO}/[CO]$ and $\lambda_{O_2}/[O_2]$ [from Austin et al. (1975)].

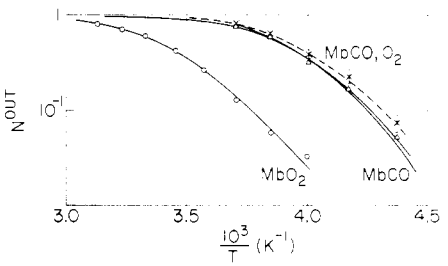

FIGURE 4: N^{out}, the fraction of the ligands that leaves the protein, vs. $10^3/T$. (○) MbO_2; (—) MbCO; (×) Mb sample with both CO and O_2; (△) fraction of MbO_2 formed.

the separate parts of the absorbance curve in Figure 2 by i–v.

Discussion

The data in Figure 2 display all of the features expected from our model. At 300 K, at i, essentially all photodissociated CO has moved out into the solvent and $N^{out} \approx 1$. The binding of O_2 is seen in ii; iii corresponds to the state MbO_2 + CO. At iv, the O_2 is slowly replaced by the CO. The binding of oxygen, characterized by a pseudo-first-order rate coefficient λ', is proportional to the O_2 concentration in the solvent. The binding of CO, shown as iv in Figure 2, occurs with an observed pseudo-first-order rate cooefficient λ''.

As the temperature is lowered below 300 K, N^{out} becomes smaller than 1 and λ' and λ'' become smaller. Direct rebinding of CO from the inside of the Mb molecule, denoted by v in Figure 2, agrees with the earlier work with MbCO (Austin et al., 1975), indicating that little O_2 is present in the part of the protein where these reactions occur. The second-order rate coefficient $\lambda'/[O_2]$ for the binding of oxygen is plotted in Figure 3 vs. $10^3/T$. Also shown in Figure 3 are the second-order rate coefficients for binding of CO and O_2 (Austin et al., 1975). The coefficients λ' and λ_{O_2} agree very well. The fraction N^{out} is given in Figure 4 as function of $10^3/T$, together with the corresponding data for MbO_2 and MbCO. Note that N^{out} is the fraction of Mb where CO leaves the protein entirely and moves into the solvent. As an example, consider T = 215 K in Figure 2, where v denotes the fraction that returns without leaving the protein. N^{out} can approximately be read off of the curve at $t \approx 10^{-2}$ s as $N^{out} \approx \Delta A(10^{-2}\text{ s})/\Delta A_{max} \approx 0.02$. Figures 3 and 4 together show that the binding of oxygen possesses an amplitude characteristic of a MbCO sample, but the time dependence of a MbO_2 sample. Also shown in Figure 4 is the fraction of MbO_2 formed, which agrees with N^{out} for

a MbCO sample. These features are in agreement with the reaction scheme shown in eq 2.

A single process, nonexponential in time, appears at temperatures below 180 K. This process is indistinguishable from process I observed earlier in pure MbCO samples (Austin et al., 1975). Process I is faster for CO than for O_2; hence, process I being unchanged does not rule out the possibility of both ligands being trapped inside the protein. To investigate this possibility, the MbO_2 intermediate was frozen by the following technique. The laser was repetitively fired at the sample at 240 K. After each flash, some of the CO leaves the protein and is replaced by O_2. The O_2 dissociation at 240 K is extremely slow (>5000 s), and consequently the sample becomes enriched in MbO_2. A sample of approximately 85% MbO_2 and 15% MbCO was obtained. The rates at 140 and 160 K were then between the values of MbCO and MbO_2. The amplitude was also smaller, characteristic of oxymyoglobin, which has a much lower quantum efficiency for dissociation than MbCO (the laser intensity was not sufficient for complete dissociation of the MbO_2). The rates are consistent with a dissociation of the mixture of MbCO and MbO_2, and do not indicate the simultaneous presence of both ligands inside the heme pocket.

To evaluate the data shown in Figure 2, we note that in our experiments $\lambda_{O_2} >> \lambda_{CO}, k_{O_2}$. Under these conditions, the scheme (eq 2) implies that the measured rates λ' and λ'' become as shown in eq 3 and 4. From the measured rate

$$\lambda' \simeq \lambda_{O_2} \tag{3}$$

$$\lambda'' \simeq (k_{O_2}/\lambda_{O_2})\lambda_{CO} \tag{4}$$

coefficients λ' and λ'', the dissociation coefficient k_{O_2} can be computed by using the previously measured values of λ_{CO} scaled to the appropriate CO concentration. The values of k_{O_2} for a 10 μM Mb sample are shown in Figure 5. The model represented by Figure 1b implies that k_{O_2} is not governed by only one barrier, but by three. We have calculated k_{O_2} by numerically solving the appropriate differential equations and using the values of activation enthalpies and entropies obtained earlier (Austin et al.,1975); the result is shown in Figure 5 as a solid line. The activation enthalpies and entropies for all steps other than A → B were determined completely by the measured MbO_2 recombination data (Austin et al., 1975). The enthalpy of step A → B was found by using the enthalpy change for the overall reaction S → A in addition to the enthalpies for the individual steps (Austin et al., 1975). The entropy was then calculated by using a known value for k_{O_2} at 293 K. The agreement between the measured and calculated values for k_{O_2} at other temperatures is surprisingly good and supports our model. In a first approximation, k_{O_2} is given by eq 5, where k_{AB}, for instance, is the rate coefficient

$$k_{O_2} = k_{AB} \frac{k_{BC}}{k_{BA} + k_{BC}} \frac{k_{CS}}{k_{CB} + k_{CS}} \tag{5}$$

for the step A → B. Values of the approximation (eq 5) are shown as a dashed line in Figure 5. Over most of the temperature range, the approximation (eq 5) provides a very good fit to the exact solution and to the data.

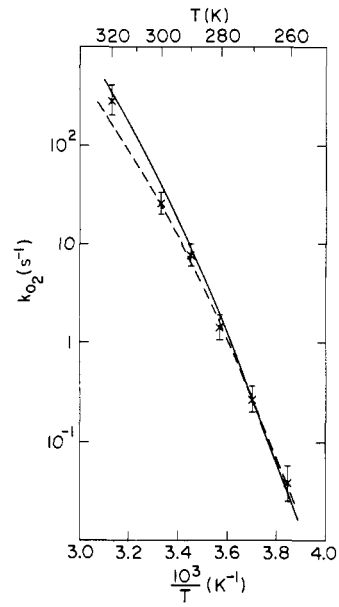

FIGURE 5: MbO_2 dissociation rates vs. $10^3/T$ as calculated from $k_{O_2} = \lambda'\lambda''/\lambda_{CO}$. k_{O_2} is the overall dissociation rate over all three barriers. The solid curve is the calculated rate using the multibarrier parameters of Austin et al. (1975). The dashed line is the approximation of eq 5. The largest contribution to the error in k_{O_2} comes from the uncertainty in oxygen concentration.

The present work shows that flash photolysis replacement experiments over a wide range of time and temperature can be helpful in separating internal from solvent reactions. Since pH (Bohr effect) and organic phosphates (Gibson, 1970a,b) predominantly change the dissociation rates of HbO_2, a method for determining these rates is desirable. Replacement reactions provide information on both the association and dissociation rates. Measurements vs. temperature will show how the influencing factor affects the ligand barriers.

References

Alberding, N., Chan, S. S., Eisenstein, L., Frauenfelder, H., Good, D., Gunsalus, I. C., Nordlund, T. M., Perutz, M. F., Reynolds, A. H., & Sorensen, L. B. (1978) *Biochemistry 17*, 43.

Antonini, E., & Brunori, M. (1971) *Hemoglobin and Myoglobin in Their Reactions with Ligands*, North-Holland Publishing Co., Amsterdam.

Austin, R. H., Beeson, K. W., Eisenstein, L., Frauenfelder, H., & Gunsalus, I. C. (1975) *Biochemistry 14*, 5355.

Austin, R. H., Beeson, K. W., Chan, S. S., Debrunner, P. G., Downing, R., Eisenstein, L., Frauenfelder, H., & Nordlund, T. M. (1976) *Rev. Sci. Instrum. 47*, 445.

Case, D. A., & Karplus, M. (1979) *J. Mol. Biol.* (in press).

Gibson, Q. H. (1959) *Progr. Biophys. Biophys. Chem. 9*, 1.

Gibson, Q. H. (1970a) *J. Biol. Chem. 245*, 3285.

Gibson, Q. H. (1970b) *Biochem. Biophys. Res. Commun. 40*, 1319.